CHARACTERISATION OF INTER-LAMINAR SHEAR STRENGTH (ILSS) OF A RESIN INFUSED WIND TURBINE BLADE POLYMER COMPOSITE VIA THE SHORT BEAM SHEAR TEST

by

MUHAMMAD HAZIQ BIN A.KADIR

10311

DISSERTATION

Submitted in partial fulfilment

of the requirements for the

Bachelor of Engineering (Hons)

(Mechanical Engineering)

MAY 2011

Universiti Teknologi PETRONAS

Bandar Seri Iskandar

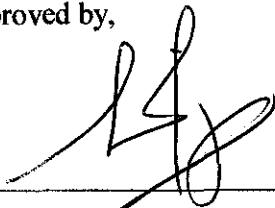31750 Tronoh

Perak Darul Ridzuan

CERTIFICATION OF APPROVAL

Characterisation of Inter-Laminar Shear Strength (ILSS) of a Resin Infused Wind Turbine Blade Polymer Composite via the Short Beam Shear Test

by

Muhammad Haziq Bin A.Kadir

A project dissertation submitted to the
Mechanical Engineering Programme
Universiti Teknologi PETRONAS
in partial fulfilment of the requirement for the
BACHELOR OF ENGINEERING (Hons)
(MECHANICAL ENGINEERING)

Approved by,

_____
(Mr. Muhammad Ridzuan Abdul Latif)

UNIVERSITI TEKNOLOGI PETRONAS
TRONOH, PERAK
MAY 2011

i

CERTIFICATION OF ORIGINALITY

This is to certify that I am responsible for the work submitted in this project, that the original work is my own except as specified in the references and acknowledgements, and that the original work contained herein have not been undertaken or done by unspecified sources or persons.

_____

MUHAMMAD HAZIQ BIN A. KADIR

ABSTRACT

Resin infusion process is the most preferred process by manufacturer to fabricate composite wind turbine blade. The application of this process affects the mechanical property of composite wind turbine blade such as interlaminar shear strength (ILSS). However the ILSS distribution for composite wind turbine blade that has unsymmetrical shape is not widely known and it needs to be quantified in order to measure the quality of the blade. The purpose of this study is to characterise the ILSS of a resin infused wind turbine blade polymer composite via short beam shear test and the map its distribution in a single blade. A composite wind turbine blade was manufactured by using resin infusion process and the resin infused in line feed from root to tip direction. The composite blade was divided into 27 blocks with 9 columns and 3 lines and a total of 6 specimens per block were cut according to ASTM Standard D2344. Universal testing machine with three point bending fixture used for the short beam shear test and the maximum load observed during test is converted into ILSS value by using ILSS equation obtained from ASTM Standard D2344. It was found that the root area of the blade has the highest ILSS followed by its middle area and root area. Moreover, the lower side of the blade has higher ILSS value compared to its upper side. The results showed that the specimen obtained from area containing low void formation has high ILSS value while area containing high void formation leads to low ILSS value. The void formation in the composite wind turbine blade influences tits ILSS distribution. As the ILSS mapping objective was achieved, the ILSS value variation among specimens obtained from the upper side of the blade is higher compared to its lower side. It proved that the ILSS value at the lower side of the blade is more consistent compared to its upper side. Several recommendations also have been discussed in this report in order to improve the methodology process and to obtain more accurate data.

ACKNOWLEDGEMENT

First of all, the author would like to express utmost gratitude and appreciation to Allah because with His blessings and help, the Final Year Project went very smoothly. Alhamdulillah, all praises to Him that the author have been able to complete this project on time.

This project would not have been possible without the assistance and guidance of certain individuals and organization whose contributions have helped in its completion. First and foremost, the author would like to express his sincere thanks and utmost appreciation to the project supervisor, Mr. Muhamad Ridzuan Abdul Latif for having faith and strong support in guiding the author throughout the whole period of completing the final year project. His kind assistance and guidance from the beginning to the end of this study really help me to undergo my project successfully.

Special express gratitude is also reserved for the Mechanical Engineering Department of Universiti Teknologi PETRONAS for providing excellent support in terms of providing cutting edge knowledge and information not just within the Final Year Project but also the five years spent undergoing every single bit of invaluable knowledge on mechanical engineering.

The author would also like to deliver his warmth appreciation to the parties who are involved with this project such as postgraduate student, Mr. Mohd Azuan and technical staff Mr. Paris for assisting with the technical support and guidance towards this project.

Finally many thanks to the author's family and fellow colleagues for their help and ideas throughout the completion of this study. I hope that the outcome of this report will bring beneficial output to others as well. Thank you very much everyone.

TABLE OF CONTENT

LIST OF FIGURES

LIST OF TABLES

CHAPTER 1

INTRODUCTION

1.1   Project Background

A wind turbine is a device for converting the kinetic energy in wind into the mechanical energy of shaft. Among of the important component in wind turbine is the blades. Wind turbine blades are subjected to static and dynamic lift, drag and inertial over a wide range of temperatures and other severe environmental such as UV light, rain, hail bird strikes and etc (Walcyk, 2010). Thus the characteristic of the wind turbine blades are high strength-to-weight ratio, corrosion resistant, high rigidity, fatigue and wear resistant. In order for the wind turbine to accelerate quickly if the winds pick up and keeping the tip ratio nearly constant, the blades must have low rotational inertia. Composite materials such as glass fibre reinforce plastic (GFRP) are widely used to construct the outer layer of wind turbine blade due to its outstanding mechanical properties. In manufacturer point of view, GFRP material is the best material used to construct the outer sin of blade as it ease to manufacture at low cost.

Nowadays, resin infusion technique is used in the industry to produce wind turbine blade polymer composite. It is a specialized advanced laminating technique that highly improves the strength and quality of glass fibre parts against conventional hand lay-up. By applying laminate engineering and resin infusion technology simultaneously allows for optimization of a part in terms of strength and weight (Nava, 2000). Different strategies can be made to manufacture this polymer composite such as by flowing resin in different feed type (line or point) and by changing direction of the resin flow (tip to root or trailing edge to leading edge). By using this technique, numerous benefits and significant strength gains are essentially due to the method of reinforcing the materials within a vacuum all at once. The tremendous clamping pressure of the vacuum (approximately 1 ton/meter square) helps fuse the materials together with any air voids

1

being replaced by resin. The advantage of this type of technology is that it allows the infusion process for close profile and sandwich arrangement material. Apart from that, the strength to weight ratio produced by this approach is impressive and it is claimed that the same tensile strength as steel is obtained but at one-quarter of the weight. In addition this technique produces low void content and reduces operator exposure to harmful emissions.

Interlaminar shear strength (ILSS) property is an indicator used to measure the quality and strength of polymer composite structures. It is the maximum shear stress existing between layers of laminated material. There are different test methods used for the evaluation of mechanical properties based primarily on strain rate required (Sierakowski et al, 1997). The short beam method (ASTM Standard D2344) is commonly employed to measure the apparent ILSS of unidirectional fibre-reinforced composite materials. A short beam specimen of rectangular in cross section is utilized, the specimen resting on two steel support cylinders that allow lateral motion, the load being applied by means of a steel loading cylinder at the centre length of the specimen. A short beam shear test using two loading cylinders to apply the load called four point shear test, is an alternative to the standard short beam shear test, which is also called the three point shear test method.

1.2   Problem Statement

Wind turbine blade must have high strength-to-weight ratio and high rigidity to withstand high force over wide range of temperature and severe environment which is very hard for it to achieve it without any reinforcement. Appropriate process need to be considered as the wind turbine blade has a curved shape, close profile and sandwich arrangement material. The process of manufacturing the glass fibre reinforced epoxy composite wind turbine blade is executed by using the resin infusion process. By using this process, the formation of void is unavoidable fact and each of the strategy produce different inclusion of the void. The inclusion of voids in the final part will have a detrimental impact on the mechanical properties of the composites such as Interlaminar Shear Strength (ILSS) even at a very low volume fraction (Samsuddin, 2010). Further

2

studies of ILSS's distribution on wind turbine blade need to be done to know the quality of current manufactured wind turbine blade.

1.3 Objective and Scope of Study

1.3.1 Objectives

The objectives of the project are:

1. To characterize the ILSS (Interlaminar Shear Strength) in a wind turbine blade polymer composite manufactured using resin infusion process via short beam shear test.

2. To map the ILSS distribution in a single blade.

1.3.2 Scope of study

This study concentrates on wind turbine blade polymer composite manufactured by using resin infusion technique. The base material of the wind turbine blade is made from wood and it is strengthen with glass fibre reinforce plastic. In resin infusion process, the resin consist of epoxy, acetone and hardener and it flows from root to tip in line feed type.

The focus of this study is in investigating the ILSS (Interlaminar Shear Strength) property of wind turbine blade polymer composite by using ASTM Standard D2344 also known as Short Beam Shear Test. The machine used in this test is the universal testing machine with three point bending fixture and all the information related such as the span length and dimension of specimen were based on this standard.

The vital part of this study is the wind turbine blade polymer composite analysis which analyzes the whole part of the blade. It covers from root to tip, trailing edge to leading edge and both upper side and lower side of the blade.

3

CHAPTER 2

LITERATURE REVIEW

2.1 Resin Infusion Strategy

The resin infusion technique operates by flowing resin from inlet to outlet across the interest area which is the wind turbine blade and glass fibre. This process can be conducted in various strategies and each strategy has different influence on the quality of the wind turbine blade. Among of the strategies are by flowing resin in different type of feed which are line feed or point feed and by changing the direction of resin flow which is from tip to root or from trailing edge to leading edge. Table 2.1 shows the strategies of conducting resin infusion process. Strategy 1 used line feed type by flowing resin from leading edge to trailing edge. Strategy 2 used points feed type by flowing resin from root to tip. Strategy 3 used lines feed type by flowing resin from root to tip. Strategy 4 used lines feed type by flowing resin from tip to root. Strategy 5 line feed type by flowing resin from trailing edge to leading edge. These entire blade already been manufactured by previous study (Jehan, 2010 et Jemaat 2011).

Each strategy influences the quality of the wind turbine blade polymer composite. By using resin infusion process, the formation of void is unavoidable fact and each of the strategy produce different inclusion of the void. The formation of void is due to entrapment of air during the formulation of the resin system, in resin rich areas, and due to moisture absorbed during the material storing and processing (Samsuddin, 2010).The inclusion of voids in the final part will have a detrimental impact on the mechanical properties of the composites such as Interlaminar Shear Strength (ILSS) even at a very low volume fraction. Costa et al (2001) reported that Interlaminar Shear Strength (ILSS) value decrease by about 34% for carbon/epoxy fabric laminates when the void content increases from 0.55% up to 5.60%, whereas Jeong (1997) reported a

reduction of 30 % for graphite/epoxy laminates made from woven fabric prepreg when the void content increases from 0 to 12% (Zhu et al, 2009).

Table 2.1: Strategies in resin infusion process (Jehan, 2010).

Strategy	Detail	Schematic
1	Line feed type From leading edge to trailing edge	Vacuum Outlet; Preform; Flow Direction; Resin Inlet
2	Point feed type From root to tip	Flow Direction; Resin Inlet; Vacuum Outlet; Preform
3	Line feed type From root to tip	Flow Direction; Resin Inlet; Vacuum Outlet; Preform
4	Line feed type From tip to root	Flow Direction; Resin Inlet; Vacuum Outlet; Preform
5	Line feed type From trailing edge to leading edge	Vacuum Outlet; Preform; Flow Direction; Resin Inlet

5

2.2 Void Content

According to Ruslan (2011), the flow front in infusion process affects the voids distribution in a wind turbine blade polymer composite. The analysis of void content performed on all part of the blade which are from root to tip, trailing edge to leading edge and both upper side and lower side of the blade. Figure 2.1 shows that, the lowest void content in the wind turbine blade polymer composite found at the inlet area (22.33%) of the infusion process followed by the middle area (25.70%) and outlet area (28.23%). At initial infusion process, the void flow smoothly causing low void content at the inlet area. As the distance and time of the flow increase, the resin is starting to jell thus causing high resistance for voids to flow. As a result, high void content will located at the outlet area compared to the inlet area of the blade.

Generally, the void content at the lower side of the blade is lower than the upper side by 12.49 – 14.17%. This is due to pressure exerted by the weight of the blade to lower side of the glass fibre causing high resistance for the void to flow along the blade. As a result low void content at the lower side of the blade compared to the upper side. However at the inlet area of the blade, lower side has higher void content compared to the upper side by 9.27%. Low permeability area at the lower side of the blade that resist the movement of void along the blade causing the void to be entrapped at the inlet area of the blade.
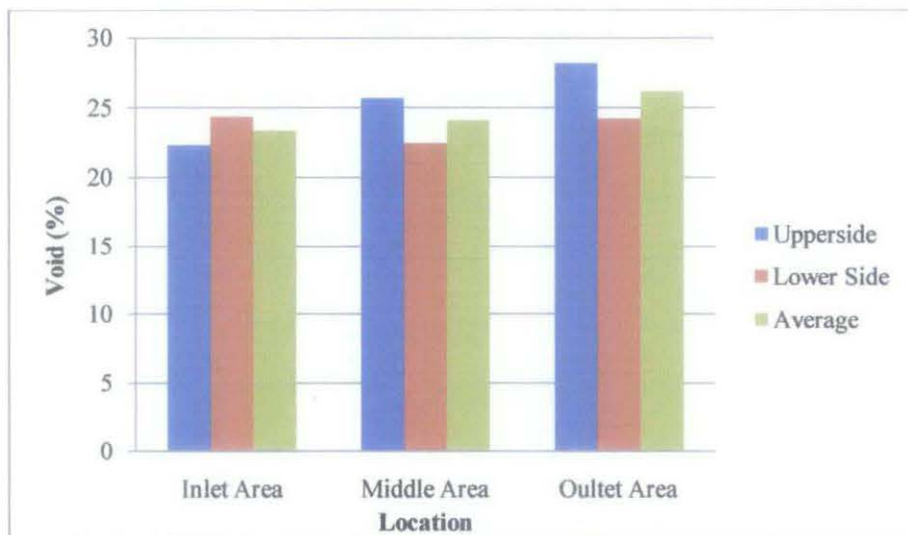
Figure 2.1: Void content of wind turbine blade polymer composite (Ruslan, 2011).

Table 2.2: Void content and interlamiar shear strength for carbon/epoxy fabric laminates and carbon/BMI fabric laminates (Michael et al, 2001).

Porosity level	Void content (%)	ILSS (MPa)	Porosity level	Void content (%)	ILSS (MPa)
Reference	0.55±0.03	82.2±3.0	Reference	0.50±0.03	79.0±1.6
EP-1	1.41±0.03	71.4±3.0	BMI-1	1.11±0.02	74.4±2.2
EP-2	1.90±0.02	67.8±1.7	BMI-2	1.60±0.03	68.8±5.5
EP-3	2.17±0.02	65.7±8.5	BMI-3	2.01±0.02	68.3±1.9
EP-4	2.18±0.02	63.5±3.7	BMI-4	2.80±0.02	66.5±4.1
EP-5	2.40±0.09	65.3±4.0	BMI-5	3.37±0.03	59.0±2.8
EP-6	4.01±0.02	59.5±3.5			
EP-7	5.60±0.03	54.5±2.8			

According to Michael et al (2001), different types of pre-impregnated materials used in the manufacturing of the laminates affect materials toughness; the processing parameters and the type of the reinforcement affect the distribution, the location, the shape and the size of the void in the laminate. Both factor, in turn, produce different effects on the mechanical properties of the composite. Two types of composite laminates were studied in this their work: carbon fabric reinforced epoxy and carbon fabric reinforced bismaleimide (BMI). Moisture was introduced by spraying water as finely and uniformly as possible to produce plate with uniform porosity. The effective pressure on the liquid resin and the amount of moisture dispersed in the laminate were used to control the porosity level. Short beam shear test used to measure the interlaminar shear strength (ILSS) of each specimen. Table 2.2 shows the value of ILSS for different void content and different composite laminate. As the void content increase in both carbon fabric epoxy (EP) and carbon fabric reinforced bismaleimide (BMI), the ILSS value of the polymer composite decrease.

Table 2.3: Summary of results for carbon/epoxy specimen (Michael et al, 1995).

Defect size (mm)		Number of	Interlaminar shear strength	C.v. (%)
Length	Height	specimen	(MPa)	
0.0	0.0	9	100.3	2.4
0.28	0.28	8	92.1	3.1
0.60	0.24	8	87.9	2.5
1.16	0.58	8	82.1	2.2
1.80	0.10	8	79.2	5.0
3.00	0.08	8	69.3	4.4

Table 2.3 shows the results for the carbon-fibre specimens. In all cases failure was due to a single crack initiating from the defect. As the size of defect increase, the interlaminar shear strength of the polymer composite decrease.

Furthermore, the fibre volume fraction also influences the interlaminar shear strength of polymer composite materials. Although there is a fair amount of scatter, there is a clear trend for the thinner specimens to have lower strength (Michael et al, 1995). In the test, a least square fitting technique is used to plot the thickness of polymer composite against the interlaminar shear strength (Figure 2.2). It is suggested that the interlaminar shear strength tending towards a constant value at high thickness because at higher thickness the variation in strength is less marked than at lower thickness.
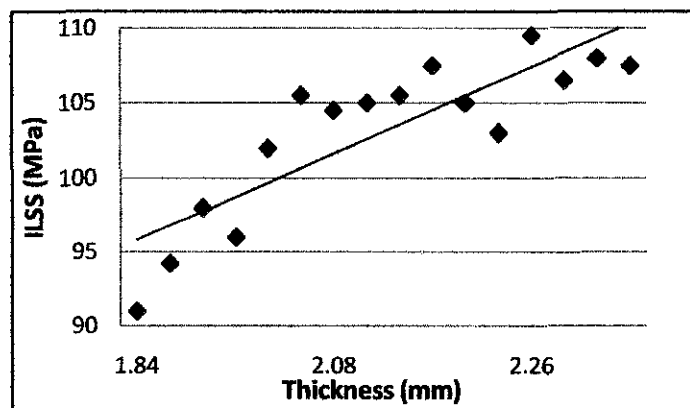
Figure 2.2: Correlation between ILSS and thickness (Michael et al, 1995).

Table 2.4: Void contents and strength for different cure pressures (Zhu et al, 2009)

Cure pressure (MPa)	Sp4-01		Sp4-02	
	Void content (%)	ILSS (MPa)	Void content (%)	ILSS (MPa)
0.4	0.6	48.2	0.4	30.1
0.1	4.9	46.4	3.5	27.8
0	6.3	45.4	4.5	27.4

According to Zhu et al (2009), the stacking sequence in manufacturing polymer composite affect the void shape and size and thus affect the composite laminate mechanical behaviour. Little work on the effect of voids on ILSS property in the literature dealt with different stacking sequences which are [([(±45)4/(0,90)/(±45)2]S (sp4-01) and [(±45)/04/(0,90)/02]S (sp4-02) lay-ups. He relates the effect of different stacking sequence and curing pressure to the formation of void sizes and shape on the ILSS as shown in Table 2.4.

Michael et al (1995) stated that fibre volume fraction affects the ILSS property. In order to prove this hypothesis, the fibre volume fraction of six untested specimens of varying thickness was measured using the resin burn-off technique. Thickness variations are often caused by resin flow during the cure. Higher thickness specimens would therefore be expected to have lower volume fraction, as shown in Figure 2.3. It also show that all the thickness variation is due to differences in the amount of resin, with a constant amount of fibres. The line is steeper than the trend from the data, indicating that some of the variation represents real difference in thickness due to varying amount of fibres and resin. As a result the ILSS tends to decrease with increasing volume fraction.
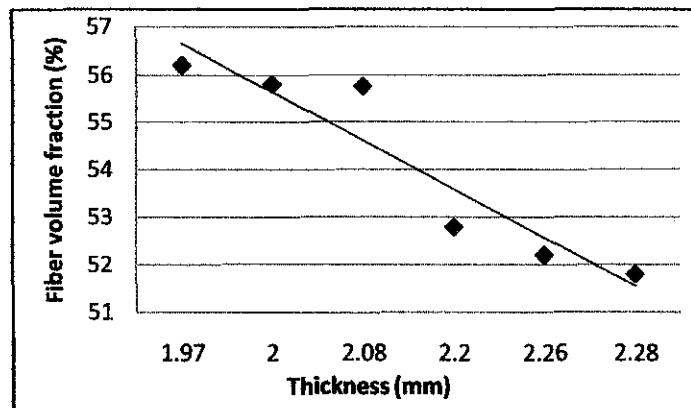
Figure 2.3: Volume fraction over thickness (Michael et al, 1995).

Table 2.5: Results for high void glass-fibre/epoxy specimens (Michael et al, 1995).

Estimated void (%)	Number of specimens	ILSS (MPa)	C.v. (%)
7	6	73.9	3.3
14	6	54.4	8.2

Table 2.5 summarized the results from the two areas of the plate with high voidage. It is assured that high void fraction material reduced strength but with different load/displacement response. A kink in the curve produced at the initiation of failure until further deformation occurred at approximately constant load, with ultimate failure occurring at much higher displacements than before. The ILSS was base on the maximum load in the first part of the response, before displacements exceeded about 0.5 mm. Figure 2.4 shows a typical response. From the results in Table 2.4 and Figure 2.4, some inference can be drawn regarding the causes of the commonly observed reduction in strength. For the glass/epoxy specimens with the smallest defect, net section stresses higher than the nominal ILSS were attained. This was possible because the reduction in cross-section only extend over a short distance. In the case of distributed voidage, the smallest net section arising from the worst combination of voids in the material may therefore not control strength. A reduction in net section over a significant distance is required in order to have an effect on strength. The average reduction in net section over the whole volume of material may therefore be a more relevant parameter. This is borne out by the strengths of the specimens with high levels of distributed voidage, which correlated with the average net section reduction. It is also consistent with the standard practice of relating ILSS to average void fraction.
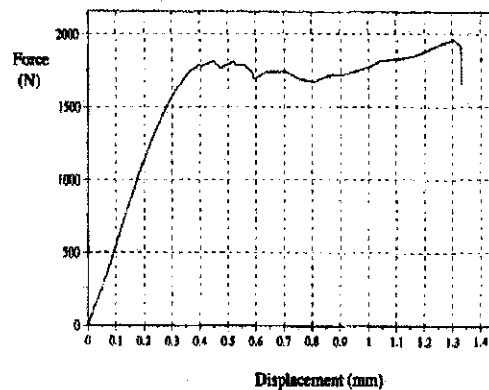
Figure2.4: Displacement responses for high void glass/epoxy (Michael et al, 1995).

10

2.3   Compression Stress

There are several limitations on the short beam shear method in conjunction with advanced composites such as graphite/epoxy. When this method used to test thin unidirectional beams, it does not usually yield interlaminar failures. Such data often reported in the literature without mentioning the failure mode, leaving the reader to believe that the desired interlaminar failure was attained (Whitney et al, 1985). Furthermore, other study proved that high shear stresses in the upper portion of the beam near concentrated load and short beam shear configuration yields stress-concentration effects which are never fully dissipated. Thus these conditions are not satisfying the principle in a highly orthotropic beam of low span-to-depth ratio.

According to the experiment and analysis made by Whitney and Browning (1985), there is evidence that compression stresses in regions where high shear-stress components exist tend to suppress interlaminar shear failure modes. Thus, initial damage in the form of vertical cracks appears to be necessary in order to induce mixed-mode horizontal interlaminar failures. For specimen without damage, the failure mode is essentially compressive buckling or yielding in the upper portion of the beam under combined compression and shear. The uniform shear stress present along a segment of the beam centre line does suggest that the apparent ILSS determined from three-point and four point (Figure 2.5) shear tests may represent minimum values. As such these methods may be useful as quality control tools. Minimum strength values are sufficient, however to use the test methods as materials screening tools.
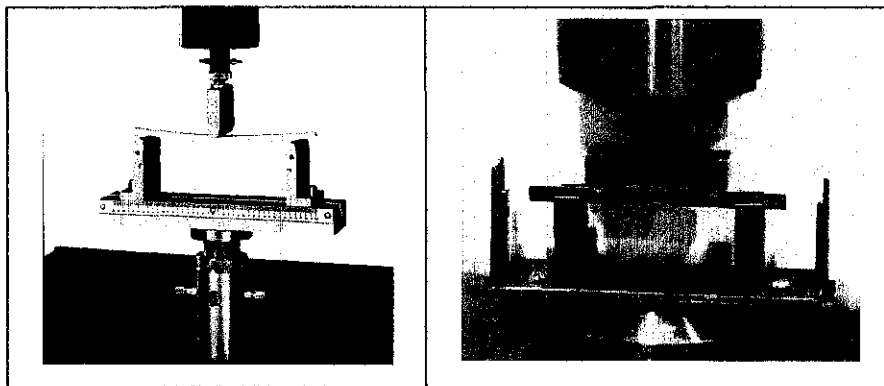
Figure 2.5: Three-point bending fixture (left); Four-point bending fixture (right)

11

CHAPTER 3

METHODOLOGY

3.1   Project Work Flow

```
                        ┌──────────┐
                       (   Start    )
                        └──────────┘
                             │
                             ▼
        ┌──────────────────────────────────────────────┐
        │  Literature review to understand the field of study │
        └──────────────────────────────────────────────┘
                             │
                             ▼
  ┌──────────────────────────────────────────────────────────────┐
  │ Manufacture wind turbine blade polymer composite by using resin infusion process │
  └──────────────────────────────────────────────────────────────┘
                             │
                             ▼
      ┌────────────────────────────────────────────────┐
      │      Prepare specimens from wind turbine blade polymer       │
      │ composite for short beam shear test according to ASTM 2344 │
      └────────────────────────────────────────────────┘
                             │
                             ▼
    ┌──────────────────────────────────────────────────────┐
    │ Test the specimens for the Interlaminar Shear Strength (ILSS) property │
    └──────────────────────────────────────────────────────┘
                             │
                             ▼
      ┌────────────────────────────────────────────────┐
      │    Map the ILSS distribution on the wind turbine blade    │
      └────────────────────────────────────────────────┘
                             │
                             ▼
          ┌────────────────────────────────────┐
          │      Compile and analyze the results      │
          └────────────────────────────────────┘
                             │
                             ▼
        ┌──────────────────────────────────────────┐
        │    Record and document the result for report    │
        └──────────────────────────────────────────┘
                             │
                             ▼
                        ┌──────────┐
                       (   End      )
                        └──────────┘
```

Figure 3.1: Project work flow

12

Figure 3.1 shows the project work flow from the literature review until the report documentation process. Several main topics were selected in the literature revie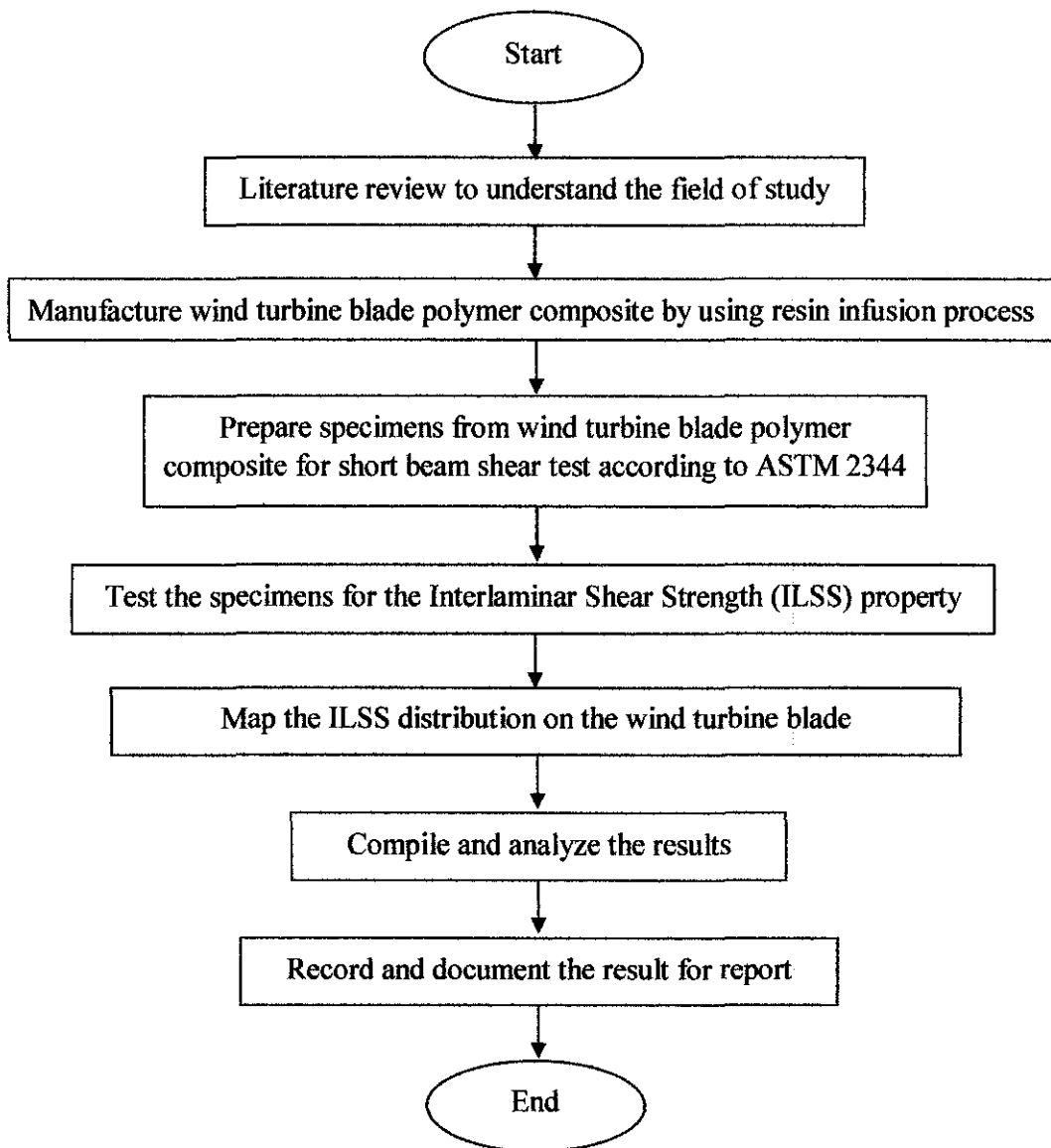w processes which are the composite wind turbine blade, resin infusion process, void formation, ILSS and short beam shear test.

Since there are several technique used in manufacturing composite wind turbine blade the best technique needs to be selected in order to produce high quality product. Resin infusion process which a specialized laminating technique was selected as it highly improves the strength and quality of fibreglass parts against conventional hand lay-up. The matrix used in this process is a combination of epoxy, acetone and hardener which then flowed in line feed from root to tip.

As the manufacturing of composite wind turbine blade finished, the next process was the sample preparation for short beam shear test process. It started with the determination of specimen number and location process. After that was the blade cutting process which divided into two parts. The first part was cutting the blade into block and the second part was cutting block into tested specimen. Each cutting process required different process and tool. In the second part, the composite material need to be peeled from the rubber wood and then cut into specimen specified in the ASTM Standard D2344. Then the entire specimens were labelled according to its position.

The methodology continued with the short beam shear test which was executed to obtain the maximum load per each specimen. The specimens were position on the universal testing machine with three point bending fixture according to the ASTM Standard D2344. It emphasized on maximum load used, span length and speed of testing. All data obtained were in load value and need to be converted into ILSS value using ILSS equation. The ILSS value for the entire specimens were calculated and recoded based on its location.

Next part was the analysis process which conducted to analyze the ILSS distribution from root to tip, from leading edge to trailing edge and both upper and lower side of the blade. The results were then discussed to determine the factors that influence the ILSS distribution along the blade. Then by using Microsoft Excel software, the ILSS distribution was mapped on a single blade based on its distance and block.

13

Finally, the conclusion was made to conclude the results obtained and to explain the objectives achievement. Several explanations on problem encountered and recommendations on improving this project have been made for future reference.

3.2 Material and Equipment

Table 3.1: Material and equipments.

Material/Equipment	Detail
Epoxy, hardener and acetone.	To act as substance for glass fibre reinforcement.
Net, breather, sealant tape, vacuum bag, resin inlet line and vacuum line.	To perform the infusion process.
Sketch tool (Pencil, ruler and marker pen)	To sketch division line on the wind turbine blade polymer composite for cutting process.
Vernier calliper	To measure the thickness of the wind turbine blade polymer composite and dimension of specimens.
Linear abrasive cutter machine	To cut the wind turbine blade polymer composite to specimen
Rotating abrasive cutter machine	To cut the polymer composite into required dimension.
Box Cutter	To remove the wood from the polymer composite.
Sand paper	To smoothen the edge of specimen and surface of specimen from wood residue.
Universal Testing Machine: Three with Three Point Bending Fixture	To measure the ILSS of the polymer composite

Table 3.1 shows the material and equipment used in this project. Understanding the safety guideline given by technician is very important because some of the equipments are dangerous such as rotating and linear abrasive cutter machine. Furthermore, there are also sophisticated equipment that needs to be handled according to the guideline due to its multifunction and delicateness.

3.3 Polymer Composite Blade Construction.

Strategy: Line feeding from root to tip

Figure 3.2: Arrangement of blade, fibre, net and breather.
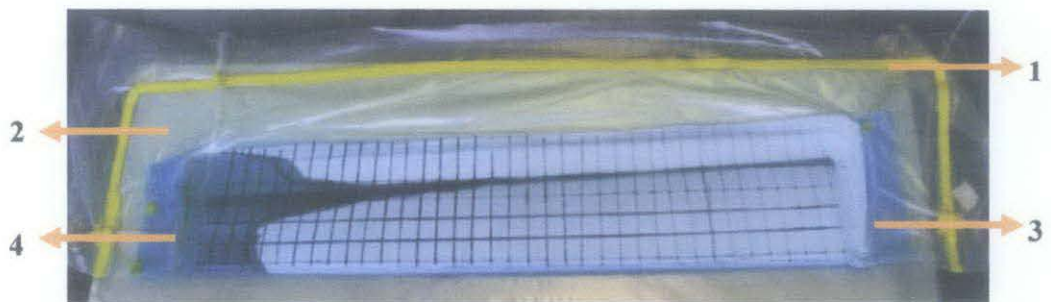

Figure 3.3: Complete set up of blade infusion process (1: Sealant tape, 2: Vacuum bag, 3: Vacuum line, 4: Resin inlet line).

15

3.3.1 Procedure:

1. The blade, fibre, breather, and net were arranged as show in Figure 3.2.

2. First spiral tubing was cut similar length of the root length and placed at the base of the blade. This is the resin inlet line.

3. Second spiral tubing was cut similar length if the tip length and placed at the tip of the blade. This is the vacuum line.

4. Vacuum bag was wrapped around to cover the whole surfaces of the blade and then sealed using sealant tape (Figure 3.3).

5. Vacuum pump was started and the air trapped inside the vacuum bag was evacuated.

6. Hissing sound from the seal around the vacuum bag and tube was checked to make sure no leak occur before resin infusion process started.

7. 80 g epoxy, 48 g hardener and 192 g acetone were then missed slowly and stirred properly.

8. The mixture was then degassed to eliminate bubble for 30 minutes.

9. Then, resin tube was placed inside the mixture. Vacuum pump was ensured off before the tube was placed inside the mixture.

10. The vacuum pump was started

11. The vacuum pump was tuned off right after the resin covers the entire blade.

12. The blade was left for curing process until the resin hardened.

13. Breather and net were removed from the blade.

Figure 3.4: Final product.

16

3.4   Specimens Number and Location.

The determination of location and number of specimens was an essential to the success of this project. Specimen is a potion or quantity of material for use in testing or study and it represents that particular material. Location of specimen is important to test large or uneven condition of material in order to obtain the property of that certain area. In this project, the determination of specimen's location was a crucial process because the desired material is a wind turbine blade which has circular shaped and uneven part. A wind turbine blade has 4 main parts which are leading, trailing, root and tip site and each of them has different shaped. As a result, the property such as the intelaminar shear strength of polymer composite used to reinforce the wind turbine blade is differing from one site to the other. As shown in Figure 3.5, the wind turbine blade polymer composite was divided into 9 columns (1-9) and 5 lines (A, a, B, b and C). The column section used to vary the position from the root to the tip while the line section used to vary the position from the leading site to trailing site.

As the number of specimens increase, the accurateness of the result will be increased. Thus it is important to have the highest number of specimen in this experiment in order to obtain satisfied result. In this project the specimens were taken from column 1 until 9 and line A, B and C which is equal to 27 specimens. Since the study covered both side of the wind turbine blade, a total of 54 specimens taken from it.
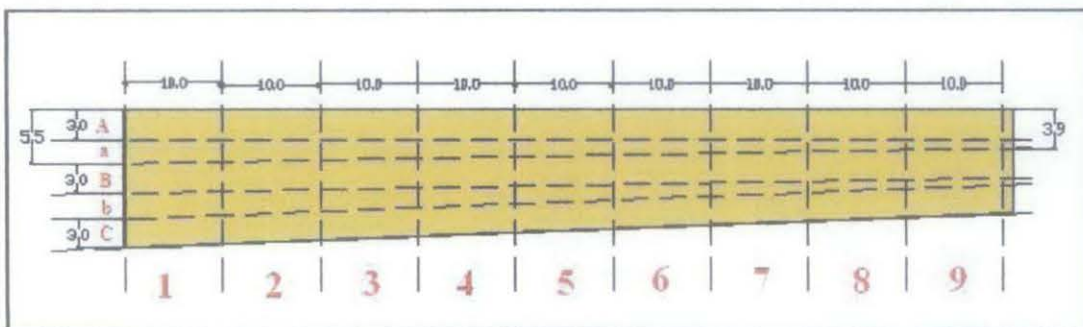

Figure 3.5: Division of blade.

17

3.5 Cutting Wind Turbine Blade Polymer Composite

Before the cutting process was started, line was sketched on the wind turbine blade polymer composite according to the specimen division (Figure 3.6). Since the cutting process will be carried out by using linear abrasive cutter machine, tolerance in sketch needs to be considered. This is due to the cutting effect of machine blade that consumes 3mm in width. If this tolerance is not considered, it will affect the integrity of dimension of the block.

Due to the lengthy in size of the wind turbine blade, the cutting process is started at its column which is in vertical direction. After that, the cutting process continued at its row which is vertical direction. During the cutting process, the feed rate of the cutting process was maintained at low magnitude in order to have a good edge finishing at each piece of the blade. Figure 3.7 shows the wind turbine blade after being cut in both vertical and horizontal direction.
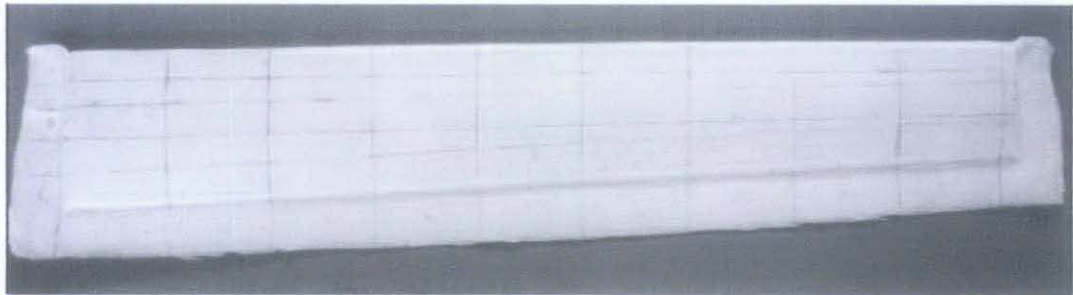

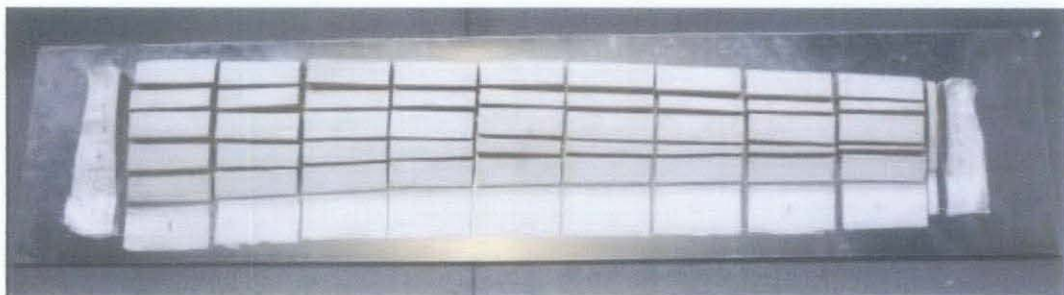**Figure 3.6: Wind turbine blade polymer composite with division line.**

Figure 3.7: Wind turbine blade polymer composite in accordance with division.

18

3.6   Specimen Thickness Measurement.

It is important to measure the thickness of cured polymer composite at different location because each location has different thickness. In this project, the measuring thickness process involved all 27 blocks of wind turbine blade polymer composite with 27 reading for the top site and 27 reading for the bottom site of the polymer composite. The divisions of the point used to measure the thickness of the polymer composite are shown in Figure 3.8.
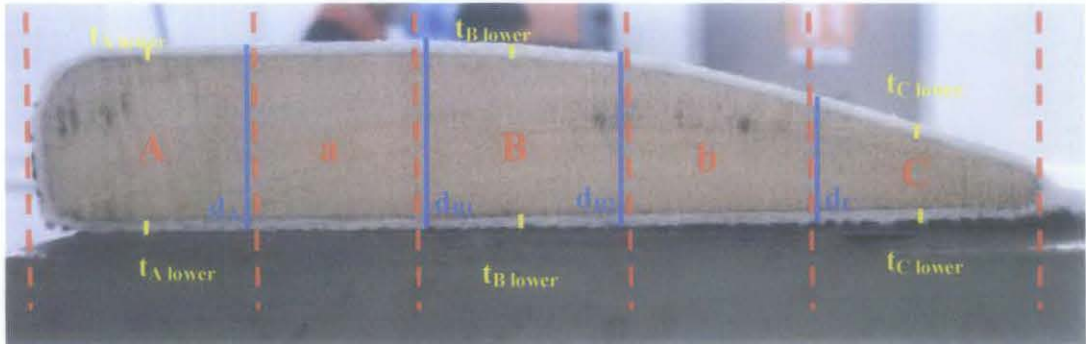

Figure 3.8: The measurement points in side view (d_A, d_{B1}, d_{B2}, d_C, $t_{A\ upper}$, $t_{A\ lower}$, t_B upper, $t_{B\ lower}$, $t_{C\ upper}$ and $t_{C\ lower}$).

3.7   Cutting Specimens.

The specimens required for testing are the polymer composite that covered the wind turbine blade at different locations. Since the polymer composite and the wind turbine blade were attached by using resin infusion process, it is difficult to separate both of them. Appropriate separation process required to separate both of them in order to maintain the integrity of the polymer composite's properties.

After the blade was cut according to the determined division (Section 3.4), the composite polymers were then separated from the wind turbine blade. The process started with cutting the polymer composite from the wind turbine blade by using linear abrasive cutter machine because it is suitable to cut small size material. The cutting process was not conducted at the line between the wood and the polymer composite because it might cut the surface of the composite and affect its integrity. Thus it conducted on the wood but nearest to the polymer composite as shown in Figure 3.9.

After the cutting process, there will be some wood residue stick to the polymer composite. This residue needs to be removed because it will influence the value of the maximum load observed during the short beam shear test. It can be removed by peeling the wood residue with box cutter as shown in Figure 3.10. This process need to be conducted gently in order to prevent any scratch to the composite polymer surface.

In order to ensure the polymer composite was free from the wood residue, it needs to be scrubbed gently with sand paper. Finally, the polymer composite was cut according to required dimension as determined by using Equation 1 and 2 (Figure 3.11).
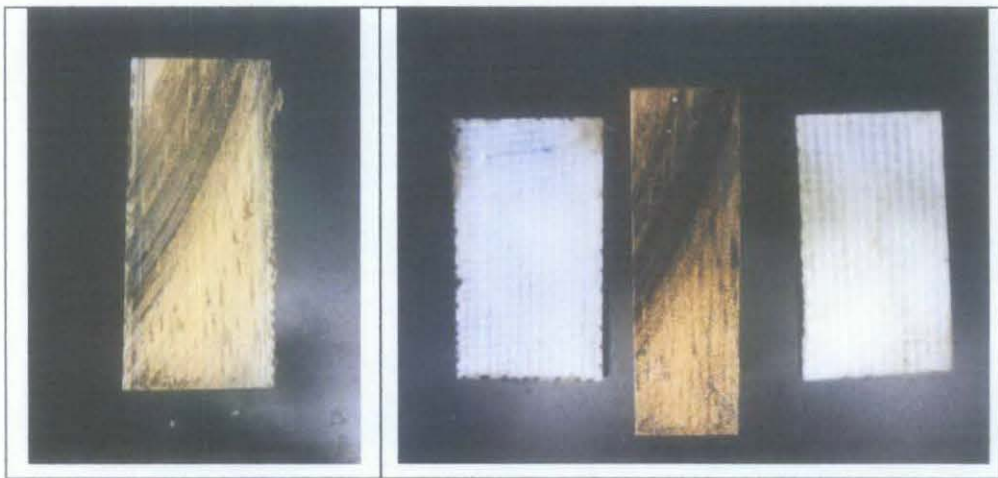

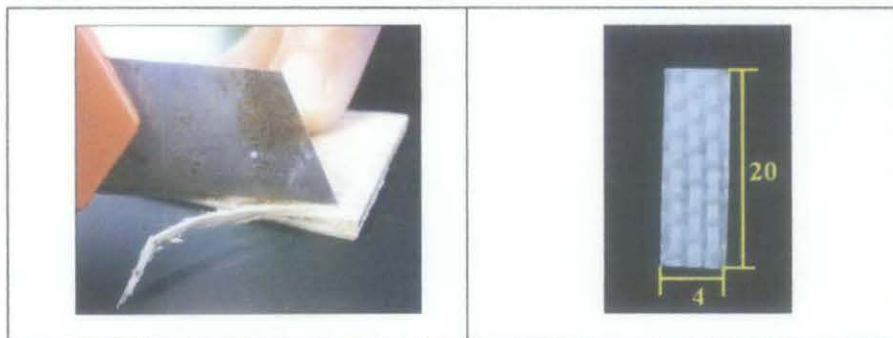**Figure 3.9: Wind turbine blade by block before cut (left) and after cut (right).**

Figure 3.10: Peeling process   **Figure 3.11: Specimen (in mm).**

3.8   Specimens Preparation.

1. Sketched the line on the wind turbine blade polymer composite according to the Figure 3.5.

2. Cut the blade by using Linear Abrasive Cutter machine in vertical direction into 9 pieces.

3. Labelled each piece of the blade starting from number 1 at the largest piece until number 9 at the smallest piece.

4. Measured the thickness of the polymer composite and the wood (d_A, d_{B1}, d_{B2}, d_C, $t_{A\ upper}$, $t_{A\ lower}$, $t_{B\ upper}$, $t_{B\ lower}$, $t_{C\ upper}$ and $t_{C\ lower}$) for each piece.

5. Cut all piece of the blade in horizontal direction using Linear Abrasive Cutter Machine.

6. Labelled each piece with A, a, B, b and C with A starting from leading side until C, the trailing side.

7. Split polymer composite from the wood blade by using Rotating Abrasive Cutter Machine for each block. Note that the polymer composite must be free from wood residue. Grind the polymer composite by using grinder if required.

8. Sketched the dimension of the required specimen according to the ASTM 2344 on the polymer composite.

9. Cut the composite into specific dimension by using Rotating Abrasive Cutter Machine. Note that the edge of each specimen must have a good finishing. Scrub the edge of the specimens by using sand paper if required.

10. Labelled all specimens according to respective line and column.

11. Measured the length width and thickness 3 times per specimen.

3.9 Short Beam Shear Test.

The short beam shear test used or ASTM Standard D-2344 used to measure the ILSS value of specimen. According to this standard, each specimen need to be verified its dimension as shown in Figure 3.12. Then the specimen was positioned on the universal testing machine with three point bending fixture where load exerted on the specimen with span length of the fixture shown in Figure 3.13. The thickness of the specimen is very important in determining its length, width and span length. ASTM Standard D2344 emphasizes on maximum load used and speed of testing. All data obtained were in load value and need to be converted into ILSS value using ILSS equation (Equation 4). The ILSS value for the entire specimens were calculated and recorded based on its location.

According to the Equation 3, the required span length is in a range of 6.4 − 8 mm. However, due to the limited span length of the fixture which the minimum value it can achieve is 16mm, the span length was fixed at that minimum value.
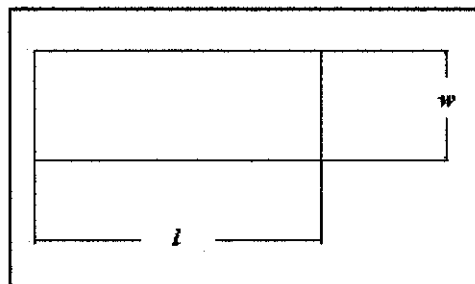

Figure 3.12: The dimension of the specimen for short beam shear test.

$$\text{Length,} \, l = \text{min span length} + \text{thickness} \times 2 \qquad (1)$$

$$\text{Width,} \, w = \text{thickness} \times 2 \qquad (2)$$

22

3.9.1 Procedure

1. Specified the specimen's geometries as shown in Figure 3.12.

2. Stored the specimen in the conditioned environment until test time.

3. Set the speed of testing at a rate of crosshead movement of 1.0mm/min.

4. If possible tested the specimen under the same fluid exposure level as that used for conditioning.

5. Monitored the test temperature by placing an appropriate thermocouple at specimen mid-length to be located on the underside of beam.

6. Inserted the specimen into the three point bending fixture, with the tool side resting on the reaction supports as shown in Figure 3.13.

7. Applied load to the specimen at the specified rate while recording data. Continue loading until either of the following occurs;

    a. A load drop-off 30%,

    b. Two-piece specimen failure or,

    c. The head travel exceeds the specimen nominal thickness.

8. Recorded load versus crosshead displacement data throughout the test method. Recorded the maximum load, final load, and the load at any obvious discontinuities in the load-displacement data.
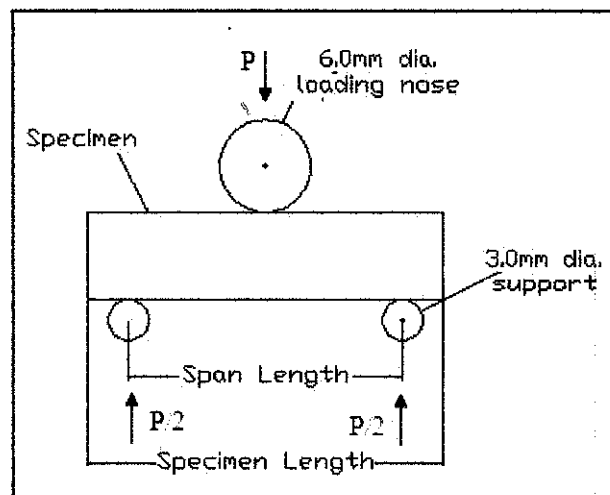

Figure 3.13: Horizontal Shear Load Diagram

$$\text{Span Length}, l_s = \text{thickness} \times 4 \tag{3}$$

23

3.9.2   Calculation

Equation 4 shows the ILSS Equation that convert the maximum load observed during the short beam shear into ILSS value. This equation uses the basic pressure equation which dividing force value with the cross section area of specimen area and multiplying it with correction factor of 0.75.

Short Beam Strength- Calculates the short-beam strength using Equation 4 as follows:

$$F^{sbs} = 0.75 \times \frac{P_m}{b \times h} \tag{4}$$

Where:

F^{sbs} = short-beam strength, MPa

P_m = maximum load observed during the test, N

b = measured specimen width, mm

h = measured specimen thickness, mm

3.10   Mapping ILSS Distribution

The purpose of ILSS distribution mapping in a single blade is to display the ILSS value of each specimen tested in a single view. By this technique, it is easier to compare the ILSS distribution between different points. The distributions were made for both upper and lower side of the blade over distance and block. Microsoft Excel software was used to tabulate the entire ILSS value of specimens. The x-axis refer to the distance and block, y-axis refers to line A, B and C while z-axis refers to the ILSS value.

CHAPTER 4

RESULT AND DISCUSSION

4.1   Polymer Composite Blade ILSS Analysis.

This section analyzes the ILSS value on section A, B and C for both upper and lower side. Appendix 2-1, Appendix 2-2 and Appendix 2-3 show the maximum load and ILSS value for section A, B and C respectively. The location column data in Appendix 2-1 refers to the division divided according to Section 3.5. Label A1.1 refers to upper side specimens while A1.2 refers to the lower side specimens and it applies to the specimens for A2 until A9. This reading is applied to the Appendix 2-2 and Appendix 2-3 in displaying the maximum load and ILSS value for Section B and Section C respectively.

Figure 4.1 show that both upper and lower side has approximately same ILSS value at the inlet (4.15MPa) and outlet area (3.25MPa). From A1 to A2, the ILSS value is increasing then it decreasing as it approaching to A9.
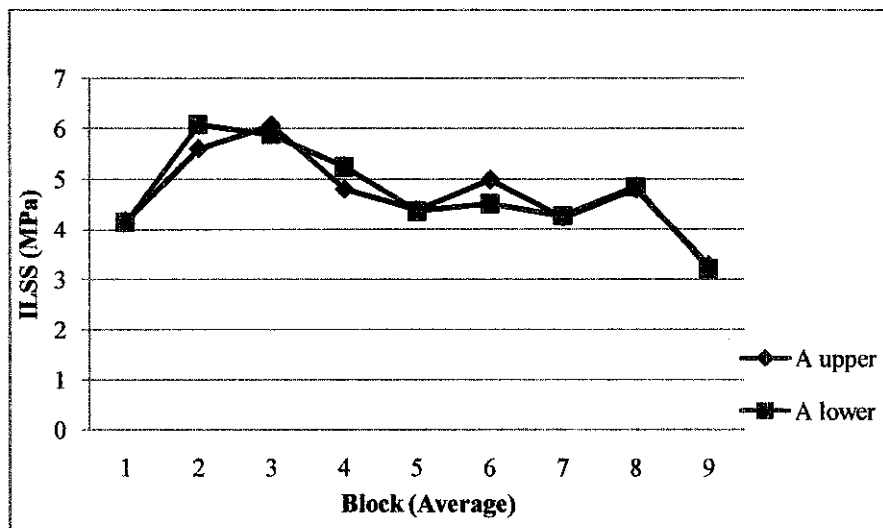
Figure 4.1: Comparison of ILSS value for upper side and lower side from A1 to A9.

Figure 4.2 shows that at lower side of the blade, the ILSS value difference between inlet and outlet is lower (0.026MPa) than the upper side (1.836MPa). As the distance approaching B9, the specimens at lower side tend to maintain its ILSS value while at upper side is decreasing.

Figure 4.3 shows that at trailing edge, the ILSS value at upper and lower side decreases less than 1MPa. However the ILSS values are unstable between the inputs and output which the highest reading at 6.799MPa and lowest reading at 4.288MPa.
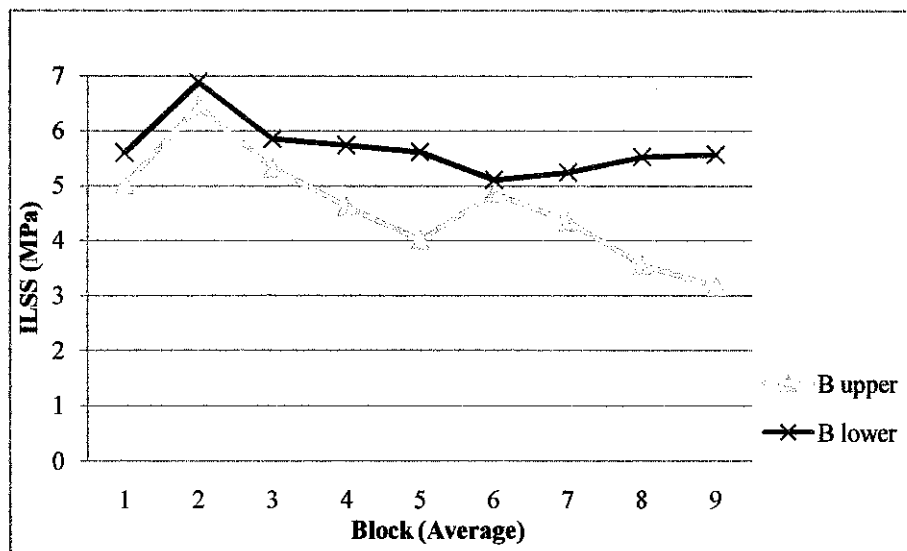
Figure 4.2: Comparison of ILSS value for upper side and lower side from B1 to B9.
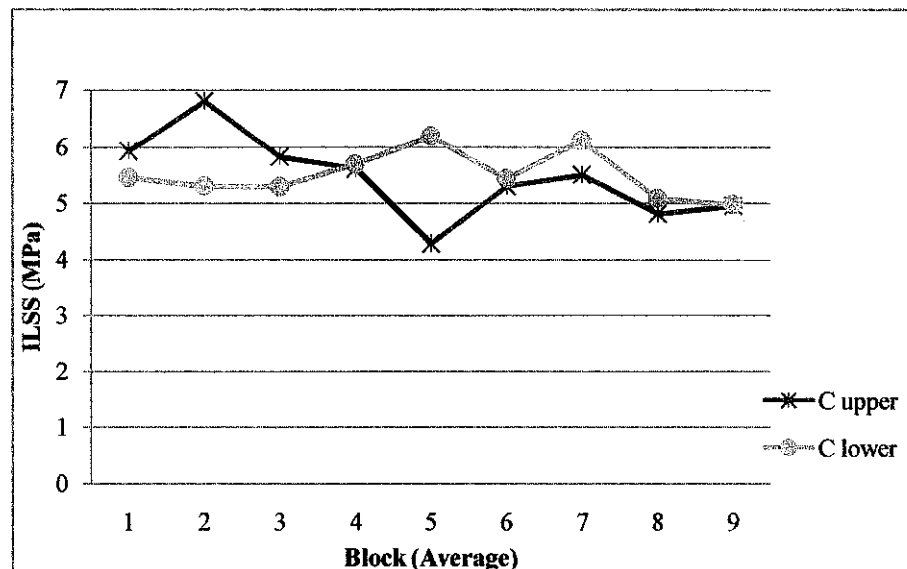
Figure 4.3: Comparison of ILSS value for upper side and lower side from C1 to C9.

Generally the ILSS value at the upper side of the blade is decreasing from root to tip as shown in Figure 4.4. The highest reading obtain for A, B and C are at A3 (6.063MPa), B2 (6.448) and C2 (6.799MPa) which located near to the inlet area. Averagely, the decrease in ILSS value from root to tip is 24.45 %.

Although the ILSS value for A, B and C at the lower sides are decreasing from root to tip, but the decreasing value is lower compared to the upper side of the blade as shown in Figure 4.5. Averagely, the inlet, outlet and decreasing ILSS value from root to tip is 5.068MPa, 4.581MPa and 9.406MPa.

Figure 4.4: Comparison of ILSS value for upper side from root to tip.

Figure 4.5: Comparison of ILSS value for lower side from root to tip.

27

4.2   ILSS Analysis from Root to Tip.

Figure 4.6 shows the relation of the average ILSS values of specimen A, B and C over division for upper and lower side of the blade. Division 1 and Division 9 signify the closest area to the inlet and outlet point of resin flows during the infusion process respectively. Each division is the average ILSS values a total of 9 specimens from section A, B and C in the same division.
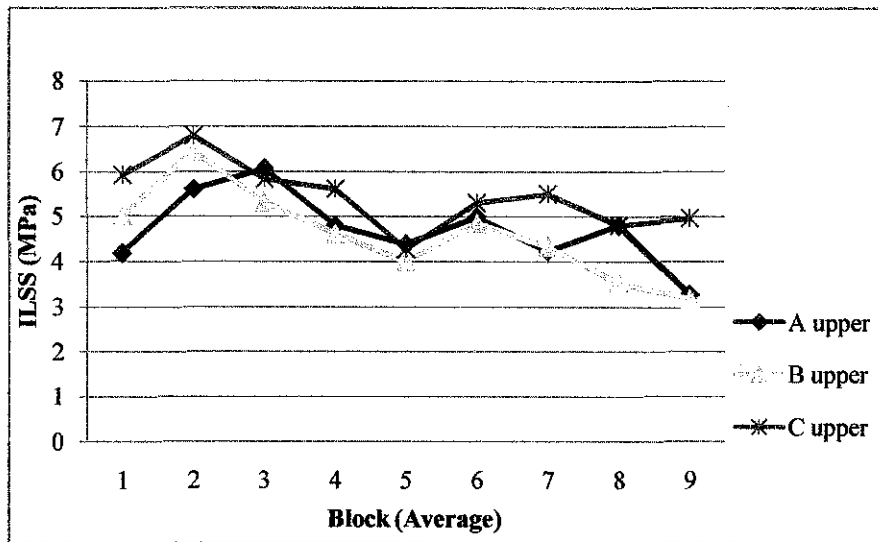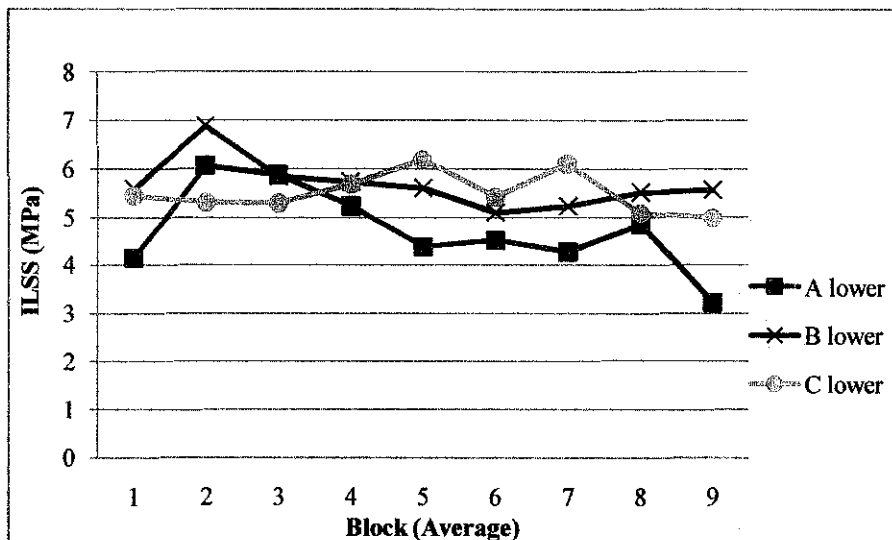
The ILSS value for the upper and lower side of the blade is increasing from Division 1 to Division 2. For the upper side the value is increasing 24.60% from 5.04MPa to 6.28MPa and 21.12% for the lower side of the blade which is from 5.07MPa to 6.09MPa. Low ILSS at Division 1 value was contributed by the high existence of void. Due to the chemical reaction, high formation of bubbles was observed during the epoxy, acetone and hardener mixing process. Although the degassing process which is used to remove the bubbles from the mixture was executed after the mixing process, there still a lot of bubble left behind in the mixture. The mixture with high amount of bubble is then sucked into the blade assembly through the inlet point. These bubbles led to the high formation of void at Division 1 which is the closest area to the inlet point and as a result reducing its ILSS value. Generally from Division 2 to Division 9, the ILSS value for the upper and lower side of the blade is decreasing.
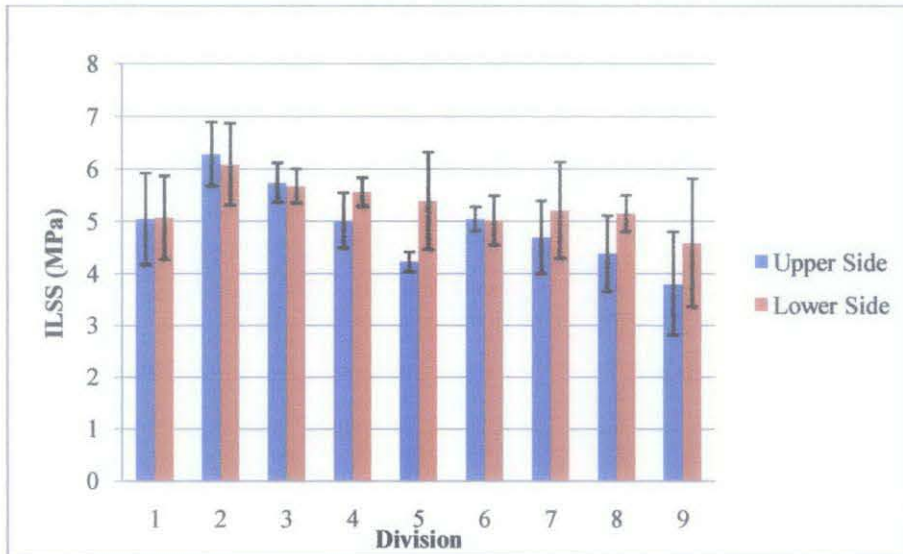
Figure 4.6: Comparison of ILSS value from root to tip.

Figure 4.7 shows the relation of the average ILSS values of specimen A, B and C over location for upper and lower side of the blade. For this analysis, the comparison made based on three different major location which are the inlet, middle and outlet area. Each area comprises of 27 specimens or three divisions starting from Division 1 to Division 3 for inlet area, Division 4 to Division 6 for middle area and Division 7 to Division 9 for outlet area. This analysis is made to obtain the overview of the wind turbine blade polymer composite ILSS distribution from root to tip.

For the upper side of the blade, the ILSS value drop 16.34% from the inlet area 5.69MPa to the middle area 4.77MPa. As the reading move to the blade outlet area, the ILSS value continues to drop 9.66% to 4.30MPa. This decreasing trend also experienced by the lower side of the blade which decrease 5.17% from inlet area (5.61MPa) to middle area (5.32MPa) and 6.20% from middle area to outlet area (4.99MPa). This result aligns with the distribution of void along the wind turbine blade. The formation of void in polymer composite decreases its ILSS value. Lowest formation void observed at the inlet area of the wind turbine blade polymer composite followed by the middle area and the outlet area. Lowest void content at inlet area gives the highest ILSS value while lowest ILSS value at the outlet area means highest void content.
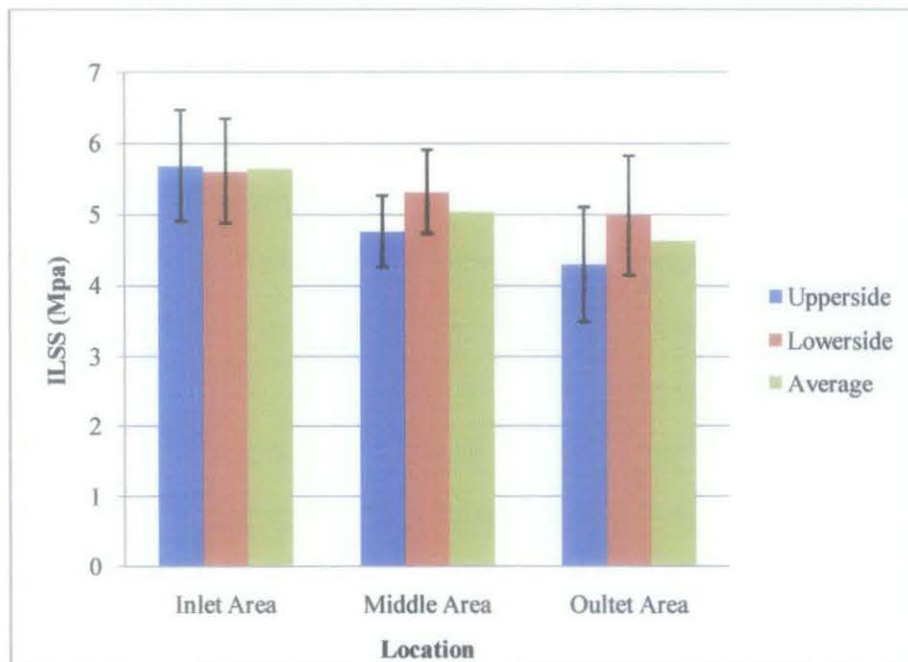
Figure 4.7: Comparison of ILSS value for inlet, middle and outlet area.

Generally, the specimens at the lower side of the blade have the higher ILSS values than the upper side by 11.71% - 15.98%. This is due to the low void content at the lower side of the blade compared to its upper side. The combination of pressure exerted by the blade weight and the lower side of the blade location which is located between the blade and the ground cause it to have low permeability area. The low permeability area at the lower side of the blade resists the movement of the bubble along the blade causing low void content. As the result high ILSS value obtained for the specimens located at the lower side of the blade. However, the same low permeability characteristic at the lower side of the blade causes the specimens at the inlet area to have lower ILSS value compared to the specimens located at the upper side by 1.41%. This is because when the mixture containing bubbles enters the blade assembly through the inlet point during the infusion process, it is more difficult for the bubbles located at the lower side of the blade to move from the inlet area to the middle area compared to the bubbles located at the upper side of the blade. This phenomenon leads to the low content of bubbles at the lower side of the blade compared to the upper side of the blade for the inlet area. As a result, for inlet area higher ILSS value for specimens located at the upper side of the blade compared to the lower side.

4.3 ILSS Analysis from Leading Edge to Trailing Edge.

Figure 4.8 shows the relation between the average ILSS values of specimen A, B and C over line for upper and lower side of the blade. For this analysis, the comparison made based on the three different major area in horizontal direction which are leading edge, intersection area and trailing edge. The leading edge covers the Section A area while intersection and trailing edge cover Section B and Section C respectively. The ILSS value for each section is the average of 27 specimens located in the same line.

Averagely as the reading moves from the leading edge to trailing edge, the specimen ILSS value is increasing from 4.72MPa to 5.14MPa until 5.48MPa. For the leading edge and trailing edge, both specimens at the upper and lower side have approximately the same ILSS value 4.72MPa ±0.01 and5.48MPa ±0.03 respectively. High variation of ILSS value occurs at the intersection area. For specimens located at the upper side of the blade, the ILSS value is the lowest (4.60MPa) while the situation is different for specimens located at the lower side is the highest (5.68MPa).
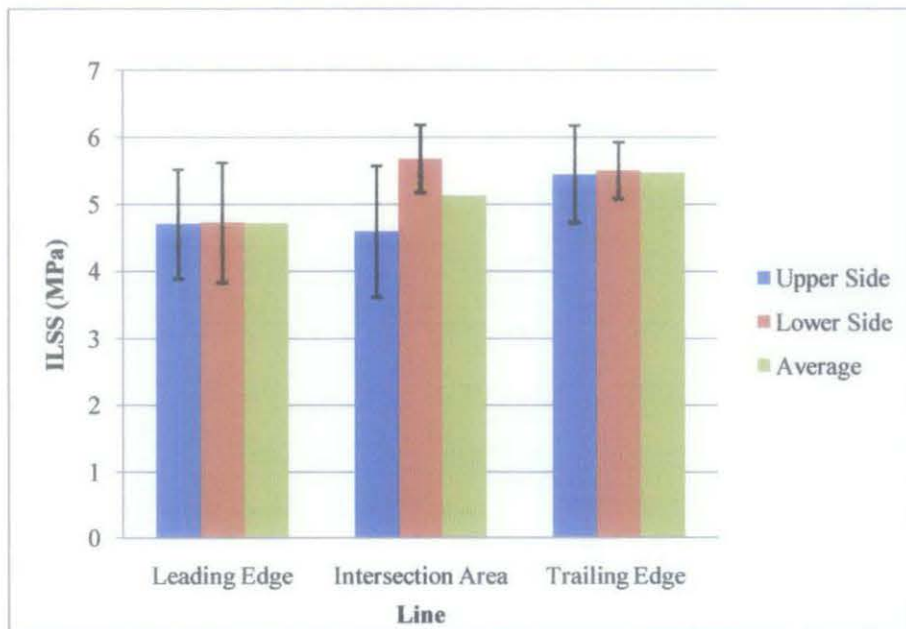
Figure 4.8: Comparison of ILSS value from leading edge to trailing edge.

The correlation between the ILSS distribution from leading edge to trailing edge results with the void distribution in the wind turbine blade polymer composite are ambiguous. According to Ruslan (2011), the void content located at intersection area is the highest for specimens located at both upper and lower side of the blade (Figure 4.9). Based on this statement, theoretically the intersection area should have the lowest ILSS value compared to the leading edge and trailing edge. This statement contradicts with the ILSS distribution from leading edge to trailing edge that indicate the leading edge has the lowest ILSS value followed by intersection area and trailing edge. Further study need to be done in order to investigate the factor influence the ILSS distribution from leading edge to trailing edge.
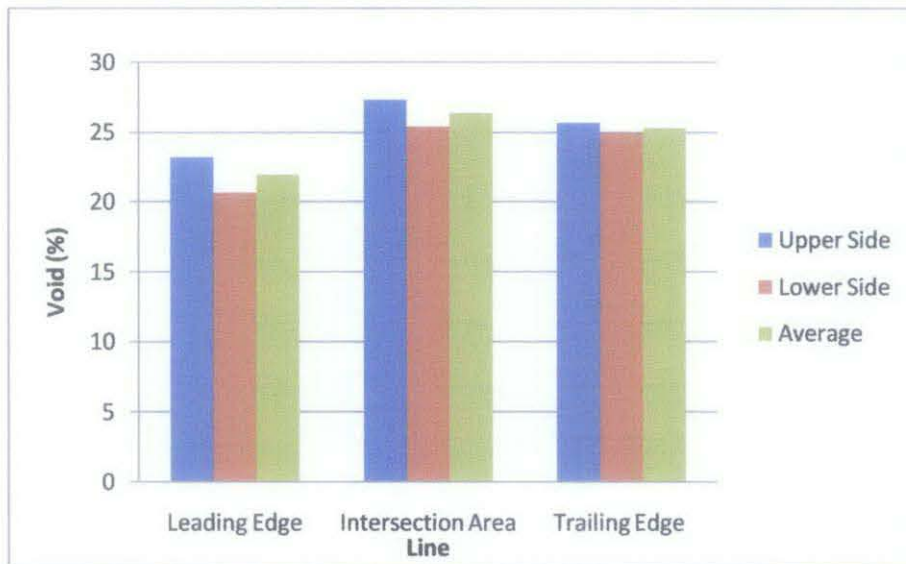

Figure 4.9: Void content distribution from leading edge to trailing edge (Ruslan, 2011).

4.4 ILSS Analysis of Section Area over Location

Figure 4.10 show the ILSS value of section area from inlet area to outlet area of the blade. The section area covers the leading edge, intersection area and trailing edge. Each of the bars is the average ILSS value of 6 specimens located from upper and lower side of the blade in a same section area.

As the location move from inlet area to outlet area, the ILSS value of all section which area leading edge, intersection area and trailing edge is decreasing. For the leading edge the highest ILSS value located at inlet area which is 5.32MPa and it has a decreasing in value of 11.84% at the middle area (4.69MPa). It continues to decrease for 12.37% at outlet area (4.11MPa). For intersection area the ILSS value at inlet area is 5.85 and it decreases (14.70%) to 4.99MPa at middle area and finally decrease (8.42%) to 4.57MPa at outlet area. Starting from 5.77MPa the trailing edge ILSS value at inlet area is decreasing for 6.07% to 5.42MPa at middle area. At outlet area the ILSS value is 5.24MPa which is less 3.32% from the middle area. The percentage of decreasing in ILSS value for trailing edge from inlet area to outlet area is the lowest compared to the intersection and leading edge.

From Figure 4.10 it is found that among three section area, trailing edge has the highest ILSS value followed by intersection area and leading area. Trailing edge has the lowest surface area followed by intersection area and leading area. At low surface area, the force distributing resin along trailing edge is high which caused the resin is flow uniformly along the surface area. As a result the difference n ILSS value from inlet area to outlet area is low compared to others section area. Furthermore, high resin force also capable in dismissing bubbles in the mixture which leads to low void content within the structure. Thus the ILSS value for trailing area is the highest compared to other section area.
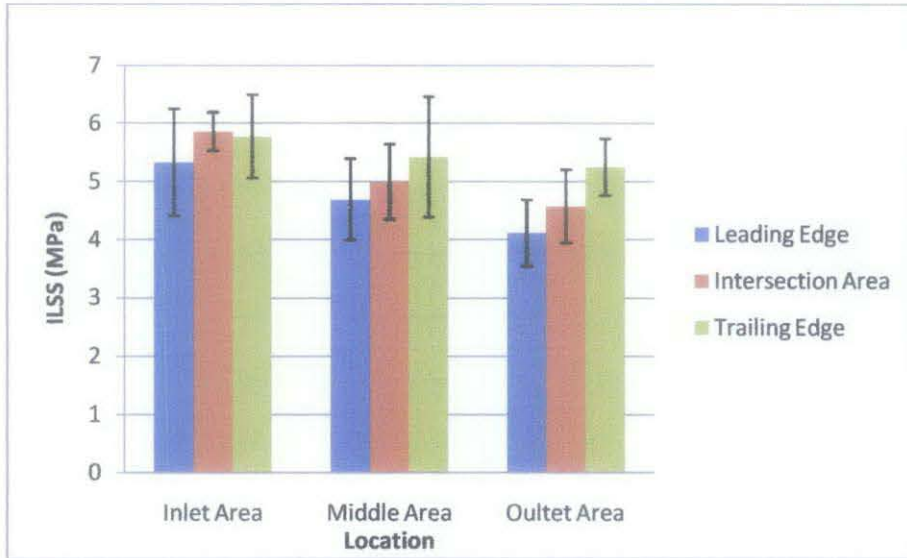
Figure 4.10: ILSS value of section area from root to tip.

4.5   Mapping ILSS Distribution on a Single Blade.

Figure 4.11 and Figure 4.12 shows the mapping of ILSS distribution for upper side and lower side for upper side and lower side of a resin infused wind turbine blade polymer composite over distance respectively. The difference of ILSS value between adjacent specimens is uneven which is some of the difference is high and some of them approaching zero. Roughly these figures show that ILSS value is higher at the inlet area compared to the outlet area of the blade.

Figure 4.13 and Figure 4.14 shows the mapping of ILSS distribution for upper side and lower side for upper side and lower side of a resin infused wind turbine blade polymer composite over division respectively. From these figures, it is clearer that the inlet area has higher ILSS value followed by the middle area and outlet area. Generally lower side of the blade has higher ILSS value compared to the upper side at every division.
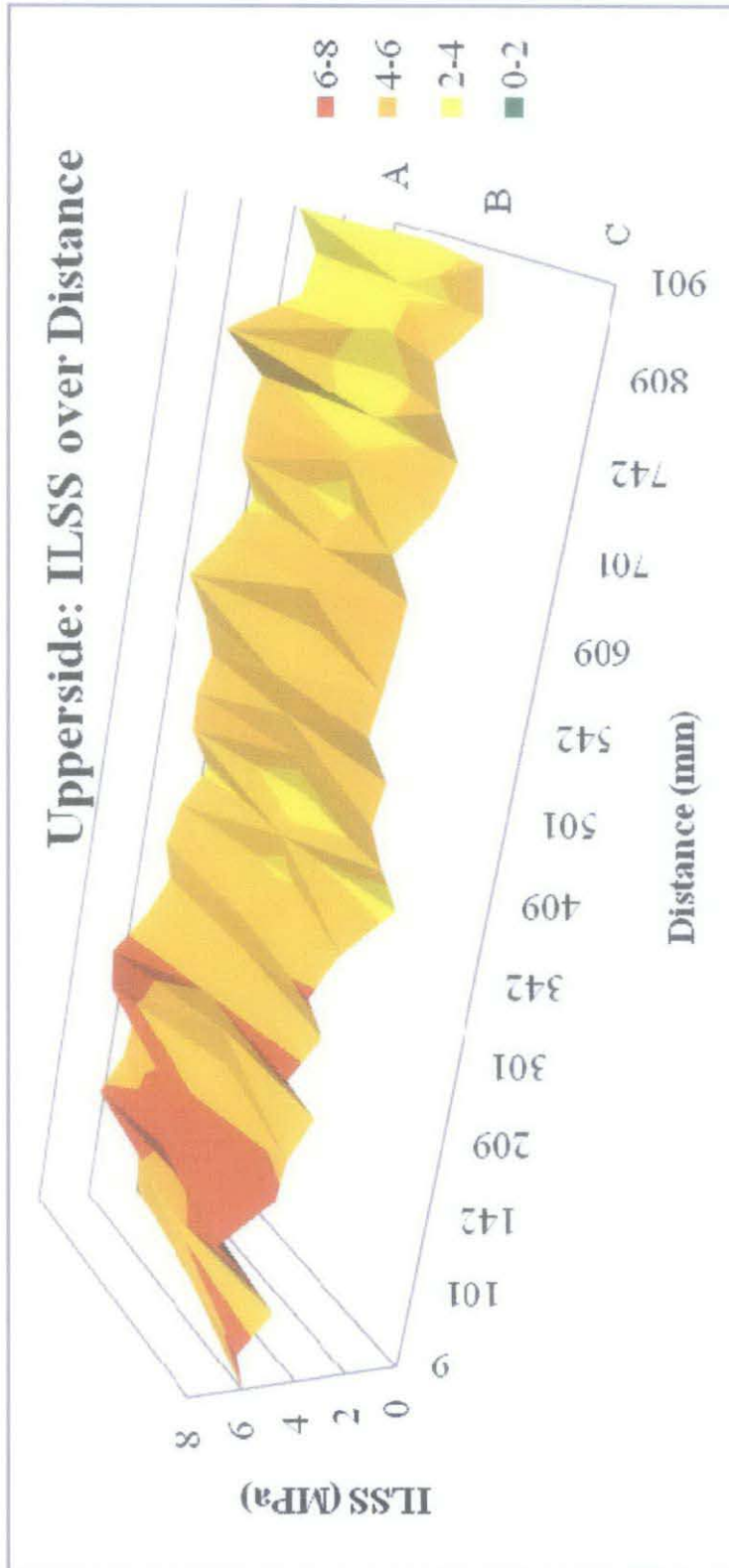
Figure 4.11: ILSS distribution for the upper side of blade by distance.
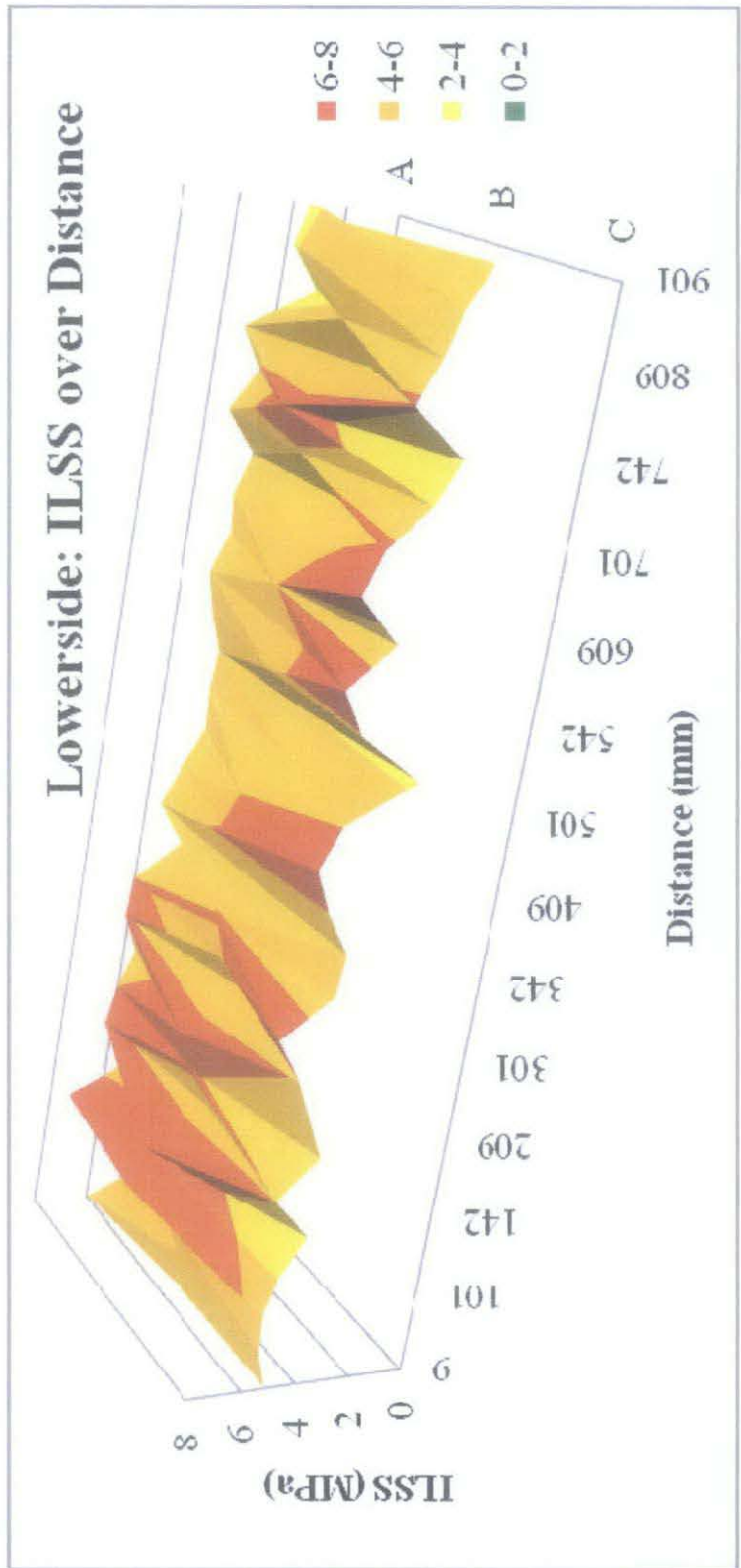
Figure 4.12: ILSS distribution for the lower side of blade by distance.
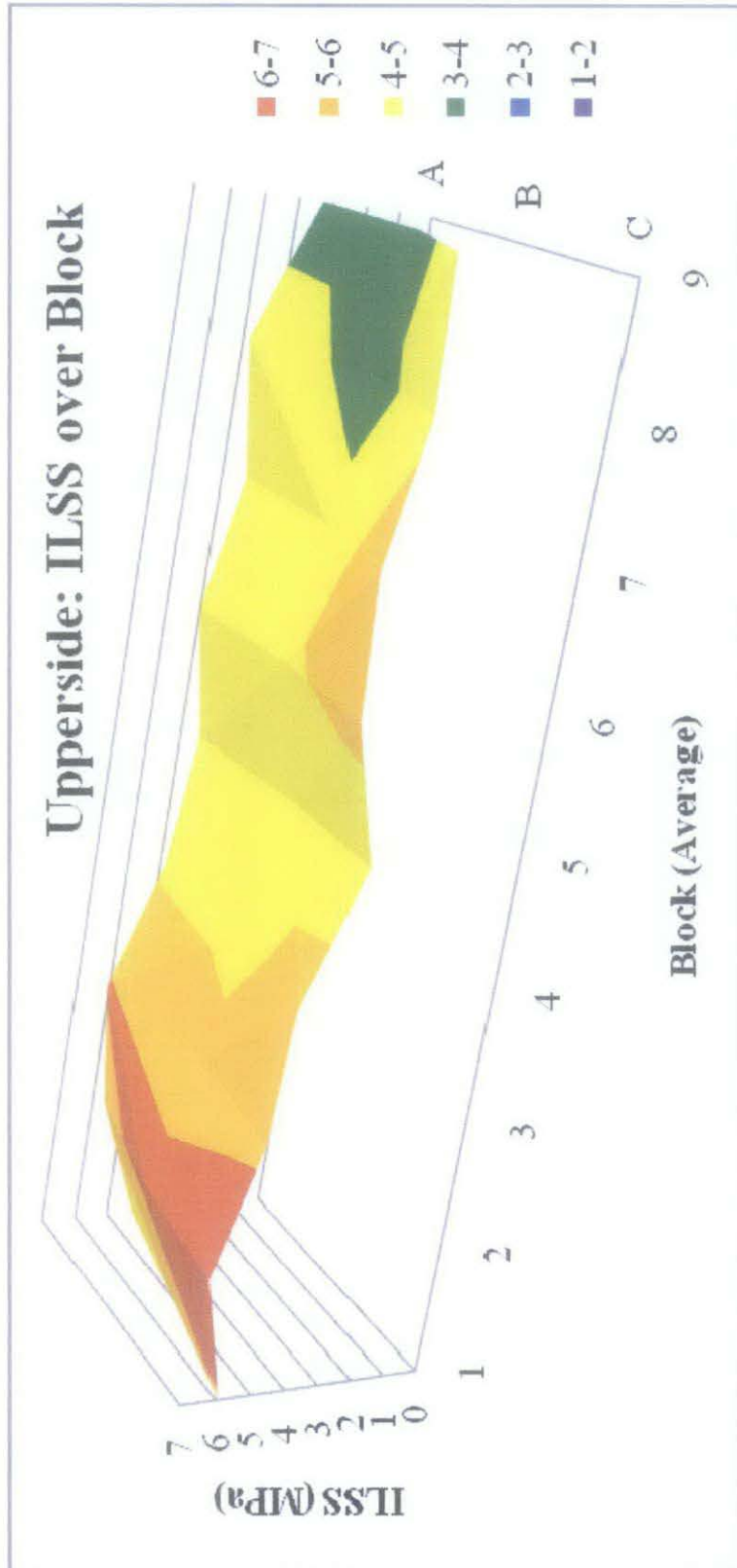
Figure 4.13: ILSS distribution for the upper side of blade by division.

37
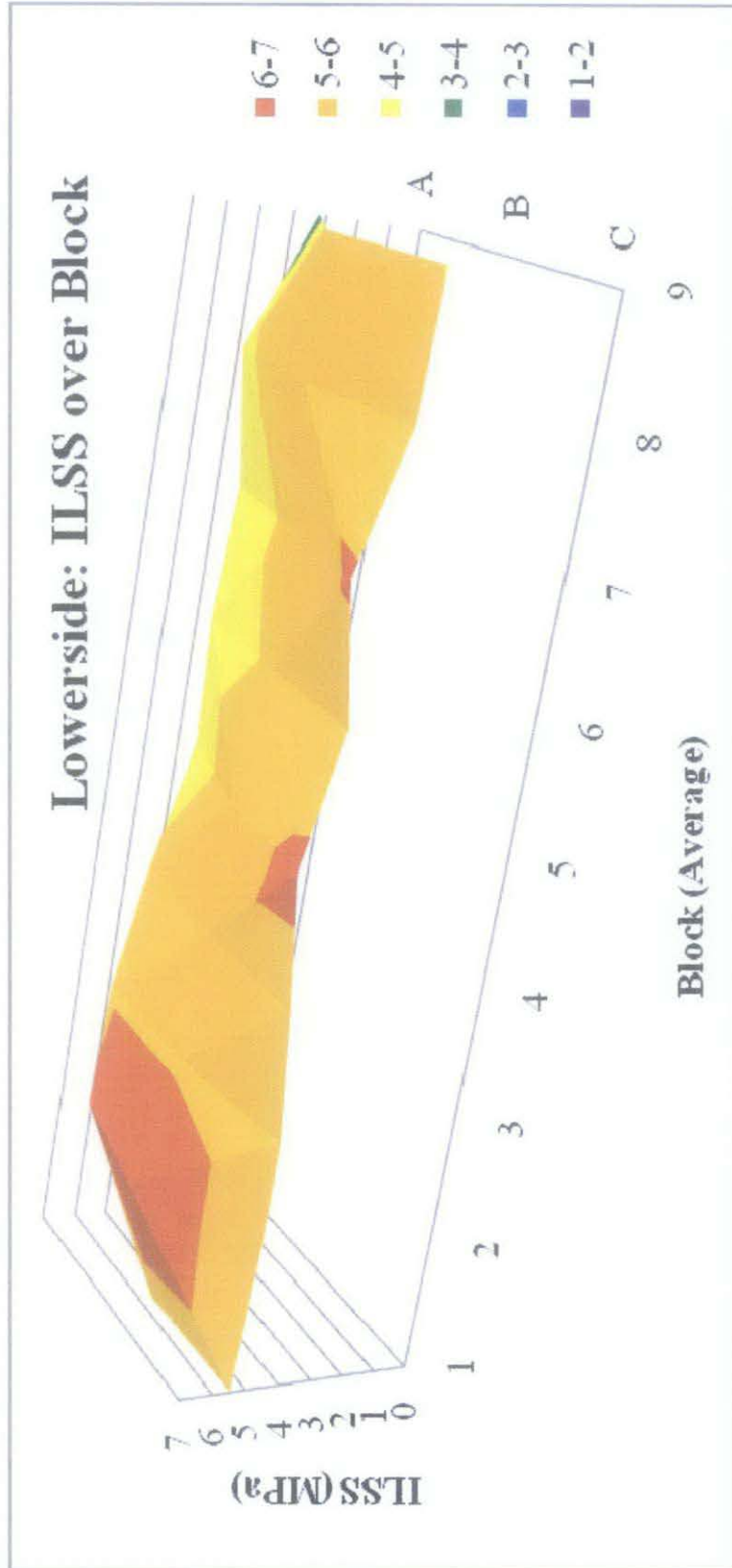
Figure 4.14: ILSS distribution for the lower side of blade by division.

CHAPTER 5

CONCLUSION AND RECOMMENDATIONS

5.1   Conclusion

The formation of void within the wind turbine blade polymer composite influences its ILSS value. High formation of void leads to low ILSS value and vice versa. As the void content at the upper side of the blade increases by 1 % its ILSS value will decrease 1%. Inlet area (root) has highest ILSS followed by middle area and outlet area (tip). The decrease in ILSS value between inlet area and middle area is higher (15.05%) compared to middle area and outlet area (9.66%). Lower side area of the blade has higher ILSS value by 8.59 % compared to its upper side. Void formation is not the only factor that influences the ILSS distribution in a single blade. The objective of mapping ILSS distribution in a single blade is achieved. The mapping done for both upper and lower side of the blade based on the division and distance of the blade.

5.2   Recommendation

For future ILSS project, smaller scale of the three point bending fixture used in short beam shear test required in order to obtain more accurate ILSS value. Separator material such as plastic required in the wind turbine blade polymer composite process. The separator need to be installed between the wood and the polymer composite so that it will be easier to separate the polymer composite from the wood during the specimen preparation process without damaging the specimen. In addition more sophisticated software is required for the mapping of the ILSS distribution in a single blade. It must not only be able to display the ILSS distribution pattern but also at exact coordinate regardless the complexity of the blade.

REFERENCES

Annual Book of ASTM Standards, 2004, Standard Test Methods for Short-Beam Strength of Polymer Matric Composite Mterials and Their Laminates, Vol. 15.03.

Costa M. L., Sergio, F.M.A., Mirabel C.R. , 2001, The Influence of Porosity on the Interlaminar Shear Strength of carbon/epoxy and carbon/bismaleimide fabric laminates, Composites Science and Technology, 61(14): 2101-2108.

Jehan S. N., 2010, Resin Infusion Strategy for Wind Turbine Blade, Final Year Report Project for Undergrad Study, Universiti Teknologi Petronas, Malaysia.

Jemaat M. R., 2011, A Comparative Study Between Two Resin Infusion Strategies in The Manufacturing of Polymer Composite Wind Turbine Blade via Resin Infusion Process, Final Repost Project for Undergrad Study, Universiti Teknologi Petronas, Malaysia.

Jeong H., 1997, Effects of Voids on the Mechanical Strength Ultrasonic Attenuation of Laminated Composites [J], Journal of Composite Materials, 31(3): 276-292.

Michael, R.W., Tom, R., Nigel, G., 1995, Reduction in Interlaminar Shear Strength by Discrete and Distributed Voids, Composite Science and Technology.

NAVA Composite Inc, 31Dec 2000 <http://www.nava.ca/infusion.htm>.

Olivier P., Cottu J. P., 1994, Ferret B. Effect of Cure Cycle Pressure and Voids on Some Mechanical Properties of Carbon/Epoxy Laminates, Composite Science and Technology.

Ruslan M. R., 2011, Characterisation of Voids in a Polymer Composite Wind Turbine Blade Manufactured via Resin Infusion Process, Final Project Repost for Undergrad Study, Universiti Teknologi Petronas, Malaysia.

Samsuddin A. S., 2010, Void Content Analysis of a Polymer Composite Manufactured via Resin Infusion Process, Final Year Project Report for Undergrad Study, Universiti Teknologi Petronas, Malaysia.

Sierakowski, R.L., Chaturvedi, S.K., 1997. Dynamic Loading and Characterization of Fiber-reinforced Composites, John Wiley and Sons Inc., New York, 15-99.

Walcyk, D., 2010, An Overview of Composite Wind Turbine Bade Manufacturing, Rensselaer Polytechnic Institute.

Whitney, J.M., Browning C. E., 1985, On short-Beam Shear Tests for Composite Material, Composite Science and Technology.

Zhu, H.Y., Li, D.H., Zhang, D.X., Wu, B.C., Chen, Y.Y., 2009 Influence of Voids on Interlaminar Shear Strength of Carbon/Epoxy Fabric Laminates, Transaction of Nonferrous Metals Society of China.

GANTT CHART (FYP_MAB 4012)

Characterization of Inter-Laminar Shear Strength (ILSS) of a Wind Turbine Blade Polymer Composite Manufactured via the Short Beam Shear Test

PROJECT GANTT CHART FOR FYP 1

No.	Activities \ Weeks	1	2	3	4	5	6	Mid semester break	7	8	9	10	11	12	13	14
1	Propose project title	X														
2	Meeting with supervisor and team members	X														
3	Preliminary Research work		X	X												
4	Collecting information from journals, research papers, etc		X	X	X											
5	Familiarize with resin infusion process				X	X										
6	Submission of Progress Report 1								X	X						
7	Studying on the Short Beam Shear Test						X									
8	Familiarizing with three point bending machine								X	X	X					
9	Preparing specimen for ILSS testing										X	X	X	X	X	
10	Seminar (compulsory)									X						
11	Submission of Progress Report 2												X	X		
12	Submission of interim report final draft															X
13	Oral presentation											study weeks				

PROJECT GANTT CHART FOR FYP 2

No.	Activities:Weeks	1	2	3	4	5	6	Mid semester break	7	8	9	10	11	12	13	14	15	16	17
1	Preparing specimen for ILSS testing	X	X	X															
3	Testing specimen for ILSS property		X	X	X														
4	Progress Report 1				X	X													
5	Analyzing obtained results					X	X		X										
6	Progress Report 2									X									
7	Seminar									X	X								
8	Compile all recorded data and information										X	X	X						
9	Discuss all data and information with supervisor												X	X					
10	Submission of final dissertation report (draft)														X	X			
11	Final oral presentation																X	X	
12	Submission of final dissertation report (final)														exam weeks				

42

Appendix 2-1: SECTION A MAXIMUM LOAD AND ILSS VALUE.

Table 4.1: Maximum load and ILSS value of specimens for A1 – A9.

Location	Max Load (N)				ILSS (MPa)			
	Specimen			Average	Specimen			Average
	1	2	3		1	2	3	
A1.1	33.865	35.652	37.438	35.652	3.969	4.178	4.387	4.178
A2.1	52.418	46.083	44.984	47.828	6.143	5.400	5.272	5.605
A3.1	53.967	55.455	45.794	51.739	6.324	6.499	5.366	6.063
A4.1	39.927	43.264	39.757	40.983	4.679	5.070	4.659	4.803
A5.1	32.462	39.686	40.167	37.438	3.804	4.651	4.707	4.387
A6.1	37.170	41.714	48.835	42.573	4.356	4.888	5.723	4.989
A7.1	38.961	31.785	37.826	36.191	4.566	3.725	4.433	4.241
A8.1	37.875	35.639	49.410	40.975	4.438	4.176	5.790	4.802
A9.1	26.917	24.713	32.444	28.025	3.154	2.896	3.802	3.284
A1.2	50.514	23.566	32.041	35.374	5.920	2.762	3.755	4.145
A2.2	62.029	40.011	53.413	51.818	7.269	4.689	6.259	6.072
A3.2	51.278	47.151	52.114	50.181	6.009	5.525	6.107	5.881
A4.2	51.484	36.350	46.336	44.723	6.033	4.260	5.430	5.241
A5.2	41.065	34.995	35.858	37.306	4.812	4.101	4.202	4.372
A6.2	34.688	38.938	41.960	38.529	4.065	4.563	4.917	4.515
A7.2	37.224	38.171	33.992	36.462	4.362	4.473	3.983	4.273
A8.2	44.159	36.446	43.474	41.360	5.175	4.271	5.095	4.847
A9.2	22.046	31.787	28.478	27.437	2.584	3.725	3.337	3.215

Appendix 2-2: SECTION B MAXIMUM LOAD AND ILSS VALUE.

Table 4.2: Maximum load and ILSS value of specimens for B1 – B9.

| Location | Max Load (N) | | | | ILSS (MPa) | | | |
| | Specimen | | | Average | Specimen | | | Average |
	1	2	3		1	2	3	
B1.1	40.073	38.147	50.251	42.824	4.696	4.470	5.889	5.018
B2.1	50.635	58.793	55.652	55.027	5.934	6.890	6.522	6.448
B3.1	41.096	44.231	50.954	45.427	4.816	5.183	5.971	5.323
B4.1	40.979	45.098	32.289	39.455	4.802	5.285	3.784	4.624
B5.1	36.106	30.146	36.489	34.247	4.231	3.533	4.276	4.013
B6.1	41.331	47.977	35.032	41.447	4.843	5.622	4.105	4.857
B7.1	40.949	38.438	31.815	37.067	4.799	4.504	3.728	4.344
B8.1	35.880	29.251	25.960	30.363	4.205	3.428	3.042	3.558
B9.1	30.808	28.800	21.874	27.161	3.610	3.375	2.563	3.183
B1.2	44.229	47.707	51.404	47.780	5.183	5.591	6.024	5.599
B2.2	66.839	64.040	45.260	58.713	7.833	7.505	5.304	6.880
B3.2	52.461	57.948	39.365	49.925	6.148	6.791	4.613	5.851
B4.2	50.089	51.556	45.215	48.953	5.870	6.042	5.299	5.737
B5.2	52.740	51.181	39.778	47.900	6.180	5.998	4.661	5.613
B6.2	34.424	49.004	47.279	43.569	4.034	5.743	5.541	5.106
B7.2	50.962	47.519	35.667	44.716	5.972	5.569	4.180	5.240
B8.2	50.077	58.116	33.360	47.185	5.868	6.810	3.909	5.529
B9.2	44.576	50.552	47.564	47.564	5.224	5.924	5.574	5.574

44

Appendix 2-3: SECTION C MAXIMUM LOAD AND ILSS VALUE.

Table 4.3: Maximum load and ILSS value of specimens for C1 – C9.

Location	Max Load (N)				ILSS (MPa)			
	Specimen			Average	Specimen			Average
	1	2	3		1	2	3	
C1.1	51.114	54.997	45.762	50.624	5.990	6.445	5.363	5.933
C2.1	55.182	67.129	51.764	58.025	6.467	7.867	6.066	6.800
C3.1	50.345	43.994	54.907	49.749	5.900	5.156	6.434	5.830
C4.1	45.995	52.977	44.814	47.929	5.390	6.208	5.252	5.617
C5.1	30.212	37.001	42.570	36.594	3.540	4.336	4.989	4.288
C6.1	40.563	48.467	46.730	45.253	4.753	5.680	5.476	5.303
C7.1	45.215	44.247	51.382	46.948	5.299	5.185	6.021	5.502
C8.1	41.270	37.160	44.885	41.105	4.836	4.355	5.260	4.817
C9.1	49.509	37.357	40.181	42.349	5.802	4.378	4.709	4.963
C1.2	43.744	47.484	48.526	46.585	5.126	5.565	5.687	5.459
C2.2	45.858	38.990	51.093	45.314	5.374	4.569	5.987	5.310
C3.2	39.715	45.211	50.707	45.211	4.654	5.298	5.942	5.298
C4.2	58.819	44.151	42.969	48.646	6.893	5.174	5.035	5.701
C5.2	51.044	56.474	51.016	52.844	5.982	6.618	5.978	6.193
C6.2	30.936	50.490	57.686	46.371	3.625	5.917	6.760	5.434
C7.2	45.082	57.944	53.580	52.202	5.283	6.790	6.279	6.117
C8.2	41.891	35.860	52.548	43.433	4.909	4.202	6.158	5.090
C9.2	46.881	43.466	37.256	42.534	5.494	5.094	4.366	4.984